Soft Matter

Accepted Manuscript

ROYAL SOCIETY OF CHEMISTRY

www.rsc.org/softmatter

Soft Matter

RSCPublishing

ARTICLE

Microdynamics Mechanism of D_2O Absorption of the Poly(2-hydroxyethyl methacrylate)-Based Contact Lens Hydrogel Studied by Two-Dimensional Correlation ATR-FTIR Spectroscopy

Cite this: DOI: 10.1039/x0xx00000x

Received ooth January 2012,
Accepted ooth January 2012

DOI: 10.1039/x0xx00000x

www.rsc.org/

Gehong Su,[a] Tao Zhou,[a,*] Yanyan Zhang,[a] Xifei Liu,[a] and Aiming Zhang[a]

A good understanding on the microdynamics of the water absorption of poly(2-hydroxyethyl methacrylate) (PHEMA)-based contact lens is significant for scientific investigation and commercial applications. In this study, the time-dependent ATR-FTIR spectroscopy combining with the perturbation correlation moving-window two-dimensional (PCMW2D) technique and 2D correlation analysis was used to study the topic of the microdynamics mechanism. PCMW2D revealed that D_2O spent 3.4 min to penetrate into the contact lens. PCMW2D also found the PHEMA-based contact lens underwent two processes (I and II) during D_2O absorption, and time regions of process I and II are 3.4-12.4 min and 12.4-57.0 min. According to 2D correlation analysis, it was approved that process I has 5 steps, and process II has 3 steps. For process I, the first step is D_2O hydrogen-bonding with "free" C=O in the side chains. The second step is the hydrogen bonds generation of O−H···O−D structure between D_2O and "free" O−H groups in the side chain ends. The third step is the hydrogen bonds generation of D_2O and the "free" C=O groups close to the crosslinking points in the contact lens. The fourth and the fifth steps are the hydration of $-CH_3$ and $-CH_2-$ groups by D_2O, respectively. For process II, the first step is the same as that of process I. The second step is the hydrogen bonds breaking of bonded O−H groups and the deuterium exchange between D_2O and O−H groups in the side chain ends. The third step is also related to the deuterium exchange, which is the hydrogen bonds regeneration between the dissociated C=O groups and the new O−D.

1. Introduction

Poly(2-hydroxyethyl methacrylate) (PHEMA) hydrogel which is synthesized from2-hydroxyethyl methacrylate (HEMA) have proven itself to be extremely promising for biomedical fields since they were first synthesized at 1960.[1] Applications of PHEMA hydrogel are versatile due to its non-toxicity, outstanding biocompatibility, and good chemical and thermal stability. Such applications include the use of PHEMA to make the contact lenses,[2] artificial corneas and skins,[3, 4] drug delivery,[5] and degradable scaffolds for tissue engineering.[6] In these applications, PHEMA hydrogels are lightly cross-linked by adding an innoxious cross-linking agent during the polymerization process of HEMA.[7]

Despite the entry of many new high-performance materials to the contact lens industry in recent few decades, the PHEMA-based contact lens still occupies a pivotal position in contact lens industry. However, its low-water retention ability and oxygen permeability has limited its long-term use in the eyes.[8] This is because the PHEMA-based hydrogel contact lens has a tendency to occur an evaporation-dehydration process in eyes.[9-11] The water at the anterior surface of the contact lens continuously evaporates into the air and draws water from the posterior surface when the eye is open. However, the water content and water-transport properties of the contact lens are probably the most important factor influencing its performance.[12] If the outward water evaporation rate is sufficiently large, and thus the contact lens exists in a state of low water content, a rubbery-to-glass transition of the contact lens would occur,[13] which will lead to discomfort and cause the lack of the oxygen supply to eyes,[14] the corneal desiccation,[15] the reduction of on-eye movement,[16] and in extreme cases the lens adheres to the corneal surface.[17]

Many works about the PHEMA-based contact lens absorbing the water were mainly focused on the water diffusion model and diffusion coefficient during the water absorption process. In general, two distinct models called the pore-flow model and the solution-diffusion model, respectively, were used to describe the solute transport through polymer membranes.[18] As for the model for describing the water transportation through

the PHEMA-based contact lens, Fatt considered the porous-flow model is suitable to describe this process.[19] However, Francesco and his coworkers argued that the solution-diffusion model provided a more consistent representation of the water transportation in the PHEMA-based contact lens,[20] and the very small pressure-induced water permeability of the PHEMA-based contact lens supported Francesco's argument.[21, 22] However, some controversy still exists. For examples, Ferrieira described three different diffusion mechanisms for the water transportation through the PHEMA-based contact lens, which depend on the crosslinking degree: a porous-flow model for a low crosslinking degree; a solution-diffusion model for a higher crosslinking degree; an intermediate mechanism at an intermediate crosslinking degree.[23] Loredana investigated the equilibrium swelling of the PHEMA with the different crosslinking degree, and he found the Ferrieira's argument was more reasonable.[24] On the other hand, the water diffusion coefficient in the PHEMA-based contact lens has been extensively studied in past two decades.[25-29] It has been widely accepted that the water self-diffusion coefficient is mainly determined by and in direct proportion to the water content in the contact lens.[25, 30, 31] Various techniques, including thermal analysis,[30] gravimetric analysis,[29] NMR,[30, 31] pulsed field gradient NMR,[25] positron lifetime technique,[33] evaporation-cell technique[20, 28] have been used to investigate the process of water diffusing through the PHEMA-based contact lens. Although the results of these characterization methods solved some problems for the water absorption of the PHEMA-based hydrogel, to the best of our knowledge, a detailed study of the microdynamics mechanism and the interaction of water with the PHEMA-based contact lens at the molecular level have been still lacked so far. Moreover, as mentioned above, a better understanding about the microdynamics mechanism and the water interaction with the PHEMA-based contact lens is significant for scientific investigation and commercial applications.

In the past decades, the time-dependent attenuated total reflection FTIR (ATR-FTIR) spectroscopy was proved to be an extremely suitable technique for studying the interaction between small molecules and polymers.[34] This method can overcome a problem called saturation artifacts when using conventional FTIR spectroscopy to study a process associated with water.[35] Therefore, the time-dependent ATR-FTIR has been widely applied to study the water absorption or the water diffusion in polymers. For example, water diffusion in many polymer materials, including LDPE,[36] PEG film,[37] positively charged PPO membrane,[38] and nafion membrane,[39] was studied using the time-dependent ATR-FTIR, and a convincing result was obtained.

Generalized two-dimensional (2D) correlation infrared spectroscopy was first proposed by Noda in 1993,[40] which has received a great attention in recent years. By using this technique, the information which cannot be readily obtained or overlapped in conventional 1D FTIR spectra will be easily captured due to the significant enhancement of the spectral resolution.[41] In addition, the sequential order of the intensity change of spectral variables can also be easily gained according to Noda's rule. Because of these two advantages, 2D correlation infrared spectroscopy has been widely used to investigate the complex chemical or physical transition processes for polymers,[42-45] and the solvent absorption process of polymer materials was also included.[36-39] In 2006, Morita proposed a new 2D correlation spectroscopy technique called perturbation-correlation moving-window two-dimensional (PCMW2D) correlation spectroscopy,[46] which is a further extension of generalized 2D correlation spectroscopy and MW2D method.[47] For PCMW2D correlation spectroscopy, the spectral correlation variation along both perturbation variables (e.g., time in the present study) and spectral variables (e.g., wavenumber) axis can be directly observed. Thus, the transition points and the transition regions can be conveniently determined from the correlation intensity along the perturbation variables' direction.

In the present study, the time-dependent ATR-FTIR spectroscopy combining with PCMW2D correlation spectroscopy and 2D correlation analysis was used to investigate the microdynamics mechanism of the water absorption of the PHEMA-based contact lens. We found that the contact lens underwent two processes during the water absorption, and the interaction between the water molecules and the functional groups in the contact lens were successfully revealed.

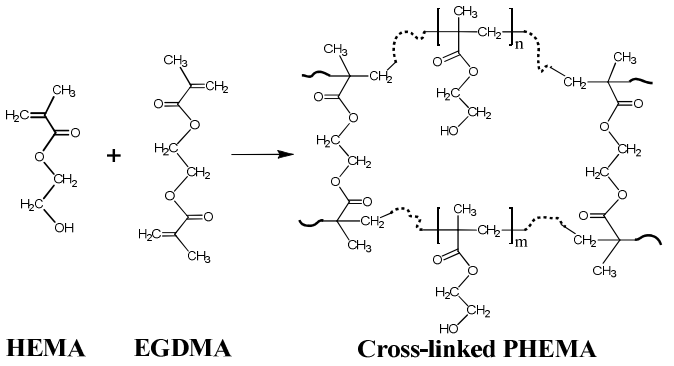

Scheme 1. Preparation of the PHEMA-based contact lens from HEMA (left) and the cross-linking agent EGDMA (middle).

2. Experimental

2.1. Materials

The PHEMA-based contact lens was purchased from Bausch & Lomb company as a commercial product. This commercial contact lens was water-saturated in a sterile isotonic solution at room temperature, and the saturated water content was 38.0 wt.%. The thickness (L_0) and the diameter (D) of the fully saturated contact lens were 40.0 μm and 13.4 mm, respectively. As shown in **Scheme 1**, the contact lens was prepared from the polymerization of HEMA with the participation of ethylene glycol dimethacrylate (EGDMA, the cross-linking agent).[48,49] Deuterated water (D_2O, D-99.9%) was purchased from Cambridge Isotope Laboratories, Inc.

2.2. Sample preparation

The PHEMA-based contact lens was immersed into plenty of distilled water for three days to remove the care solution absorbed in the contact lens. The used distilled water was changed every hour to make sure the care solution was completely removed. Then, the contact lens was carefully sandwiched between two polytetrafluoroethylene (PTFE) plates and kept in a vacuum oven for 5 days at 110 °C to fully remove absorbed water. The glass transition temperature of this dry contact lens is 116 °C (DSC), and the thickness was approximately 20 μm.

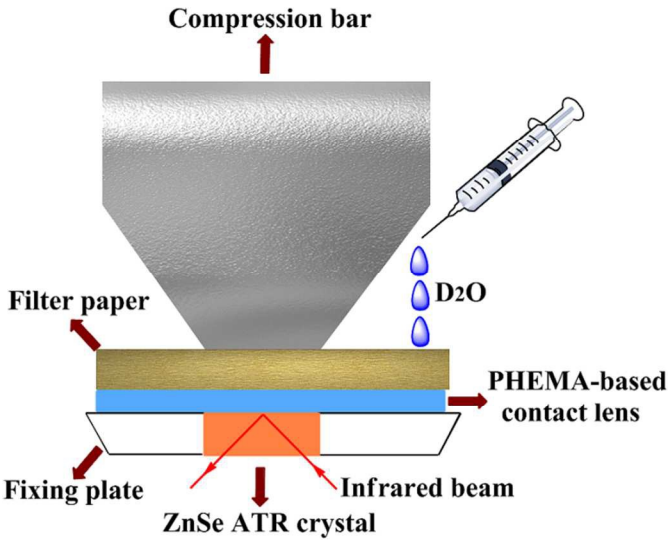

Figure 1. Schematic illustration of the time-dependent ATR-FTIR experiment.

2.3. Time-dependent ATR-FTIR of the water absorption

The time-dependent ATR-FTIR experiment was carried out at 25 °C using ATR accessory with ZnSe IRE-ATR crystal. Nicolet iS50 Fourier transform spectrometer equipped with a deuterated triglycine sulfate (DTGS) detector was used. Before the ATR-FTIR experiment, the dry contact lens was carefully sandwiched between the ZnSe crystal and a piece of filter paper, and then mounted on the ATR accessory (**Figure 1**). After that, heavy water (D_2O) was injected into the filter paper, and the time-dependent ATR-FTIR spectra in the region 4000-650 cm^{-1} were collected after 5 s. Here, the time to start collecting ATR-FTIR spectra was recorded as 0 min. In this study, the resolution of ATR-FTIR spectra was 4 cm^{-1}, and 20 scans were used for each spectra. The time-dependent ATR-FTIR spectra were collected for 60 min, and there were totally 141 FTIR spectra were obtained. The time interval between two adjacent ATR-FTIR spectra was 25.0 seconds.

Here, the heavy water (D_2O) was used instead of the distilled water in the time-dependent ATR-FTIR spectra. As everyone knows, the ordinary water presents a FTIR peak in the region 3600-3150 cm^{-1}, which is assigned to the stretching vibration of hydroxyls (O−H). As shown in **Scheme 1**, the cross-linked PHEMA also has many O−H groups which also show an overlapped broad FTIR peak in the region 3600-3150 cm^{-1}. Fortunately, the absorption peak of the stretching vibration of hydroxyls (O−D) in D_2O is within the region of 2630-2400 cm^{-1}, and the FTIR absorption peaks of the contact lens in the region of 3600-3150 cm^{-1} would not be covered up by D_2O.

2.4. Two-dimensional correlation ATR-FTIR spectroscopy

PCMW2D and the generalized 2D correlation FTIR spectra were processed, calculated, and plotted by 2DCS software, developed by one of the authors. The linear baseline corrections were applied in the regions of 3700-2800 cm^{-1}, 2700-2200 cm^{-1}, and 1800-1500 cm^{-1}. The linear baseline correction can preserve the peak shape and the intensity distribution to the maximum extent. The window size of PCMW2D was selected as 15 (*2m+1*) to produce high-quality 2D correlation spectra. The 4% correlation intensity of 2D correlation spectra was regarded as noise and was cut off. In 2D correlation FTIR spectra, the pink areas represent positive correlation intensity, while the sky blue areas represent the negative correlation intensity. The theory of PCMW2D and generalized 2D correlation spectroscopy can refer to the literature.[40,41,46]

3. Results and discussion

3.1. Time-dependent ATR-FTIR spectroscopy

As mentioned above, D_2O was used instead of H_2O to avoid the overlap between the ν(O−H) band (3600-3150 cm^{-1}) of H_2O and that of the PHEMA-based contact lens. The time-dependent ATR-FTIR spectra for D_2O absorption of the PHEMA-based contact lens in the regions of 3690-2770 cm^{-1}, 2760-2200 cm^{-1}, and 1780-1550 cm^{-1} are shown in **Figure 2**. For clarity, not all the spectra are plotted. The bands assignments and the corresponding explanations are listed in **Table 1**.

In **Figure 2(a)**, the broad bands within 3600-3150 cm^{-1} is attributed to the stretching vibration of the hydroxyl groups (O−H) in the side chains of the PHEMA-based contact lens. The region of 3050-2800 cm^{-1} is the stretching vibration of the alkyl groups. Within 3050-2800 cm^{-1}, two bands at 2990 cm^{-1} and 2948 cm^{-1} were observed. The assignments of these two bands are not reported before. However, it was reported that the bands of 2960 cm^{-1} and 2922 cm^{-1} are assigned to the asymmetric stretching vibration of dehydrated $-CH_3$ and $-CH_2-$ groups, respectively.[50] According to the literatures, the bands of the hydrophobic alkyl groups would shift to a higher wavenumber when surrounded by the water molecules, and the more water molecules surrounded, the higher wavenumber of the C−H stretching vibration presented.[51, 52] In this study, the alkyl groups of the PHEMA-based contact lens was dehydrated before ATR-FTIR experiment. However, after D_2O penetration into the contact lens, the hydration process of these hydrophobic alkyl groups immediately takes place. Consequently, the peaks of $-CH_3$ and $-CH_2-$ groups shift to a higher wavenumber. Thus, the bands at 2990 cm^{-1} and 2948 cm^{-1} are attributed to the hydrated $-CH_3$ and $-CH_2-$ groups, respectively.

Table 1. ATR-FTIR bands assignments of the PHEMA-based contact lens and D_2O.

Wavenumber(cm^{-1})	Assignments	Explanations
3600-3150	ν(O−H)	O−H stretching vibration of hydroxyl groups in the PHEMA-based contact lens
2990	ν_{as}(−CH_3, hydrated)	C−H asymmetric stretching vibration of hydrated −CH_3 in the contact lens
2948	ν_{as}(−CH_2−, hydrated)	C−H asymmetric stretching vibration of hydrated −CH_2− in the contact lens
2630-2400	ν(O−D)	O−D stretching vibration of D_2O
1723	ν(C=O, free)	C=O stretching vibration of "free" carbonyl groups in the contact lens
1703	ν(C=O, bonded)	C=O stretching vibration of hydrogen-bonded carbonyl groups in the contact lens
1660-1610	δ(O−H)	O−H bending vibration of hydroxyl groups in the contact lens

As shown in **Figure 2(a)**, it can be clearly observed that the intensity and the width of the bands within 3600-3150 cm^{-1} (attributed to O–H) gradually decreases and narrows with the time increasing from 0 to 60 min. At the same time, this bands also shifts to the high wavenumber (approximately 40 cm^{-1}). In the past decades, scientists summarized that the intensity and width of the bands of O−H stretching vibration would reduce and narrow, and the bands also moved to the high wavenumber, when the breaking of hydrogen bonds between O−H and other hydrogen bond acceptors occurred. Here, the bands change features of O–H in the contact lens is just the same as above. Therefore, it shows the gradual hydrogen bonds breaking of O–H in the PHEMA-based contact lens with D_2O diffusing in.

In **Figure 2(b)**, the bands of 2630-2400 cm^{-1} is assigned to the stretching vibration of the hydroxyl (O−D) in D_2O, and the adjacent region 2380-2280 cm^{-1} is the unavoidable bands of CO_2 in the air during the experiment. Although the bands of CO_2 is partly overlapped with that of D_2O, it has no impact on our analysis. The region of 1780-1680 cm^{-1} is assigned to the C=O stretching vibration of the PHEMA-based contact lens, and 1660-1610 cm^{-1} is attributed to the O−H bending vibration of O−H groups. In 1780-1680 cm^{-1}, the bands at 1723 cm^{-1} and 1703 cm^{-1} are attributed to "free" C=O groups and hydrogen-bonded C=O groups, respectively.[53] The bands within 3690-2770 cm^{-1}, 2760-2200 cm^{-1}, and 1780-1550 cm^{-1} can be conveniently used to describe the interactions between D_2O and O−H groups, C=O groups, and alkyl groups of the contact lens. In addition, the spectral intensities within these three spectral regions are strong enough. This gives a high signal to noise ratio, which will bring a more precise and robust result of 2D correlation analysis in the next section.

As the time extends (0-60 min), the bands intensity of O−D in D_2O gradually heightened, which clearly reveals a plenty of D_2O penetrating into the contact lens. It is also clearly observed that the intensity of 1723 cm^{-1} ("free" C=O) decreases, and that of 1703 cm^{-1} (hydrogen-bonded C=O) gradually increases, which indicates some of "free" C=O groups in the contact lens transforms into hydrogen-bonded C=O groups when D_2O continuously penetrates into the contact lens. Because the hydrogen bonds can be rapidly formed between D_2O and C=O, this phenomenon certainly comes from the formation of hydrogen bonds between D_2O and "free" C=O in the contact lens. In addition, the bands intensity of 1660-1610 cm^{-1} (δ(O−H)) gradually reduces from 0 to 60 min, whose feature is similar with that of 3600-3150 cm^{-1} (ν(O−H)) in **Figure 2(a)**, also revealing hydrogen bonds breaking of O–H groups in the contact lens in the presence of D_2O.

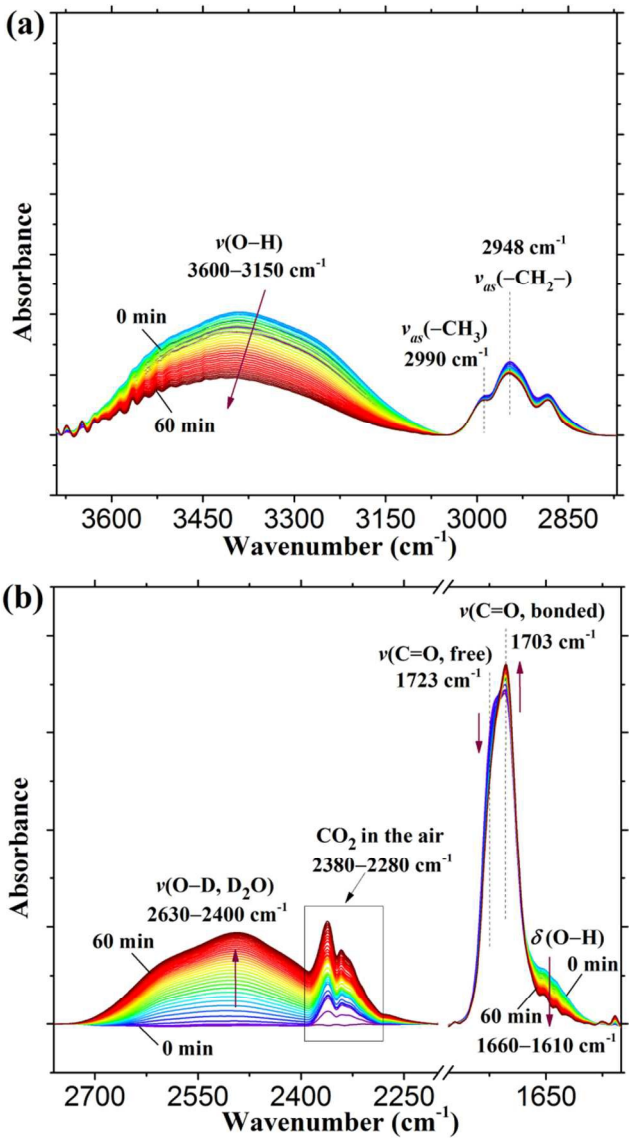

Figure 2. Time-dependent ATR-FTIR spectra measured during the water absorption of the PHEMA-based soft contact lens. **(a)** 3690-2770 cm^{-1}; **(b)** 2760-2200 cm^{-1} and 1780-1550 cm^{-1}.

Although some useful information on the D_2O diffusion into the PHEMA-based contact lens is gained from the time-dependent ATR-FTIR spectroscopy, the detail process of the interaction (e.g., the time, steps) between D_2O molecules and the PHEMA-based contact lens are still unclear. Thus, we

resort to the powerful PCMW2D and generalized 2D correlation spectroscopy to find out these key issues.

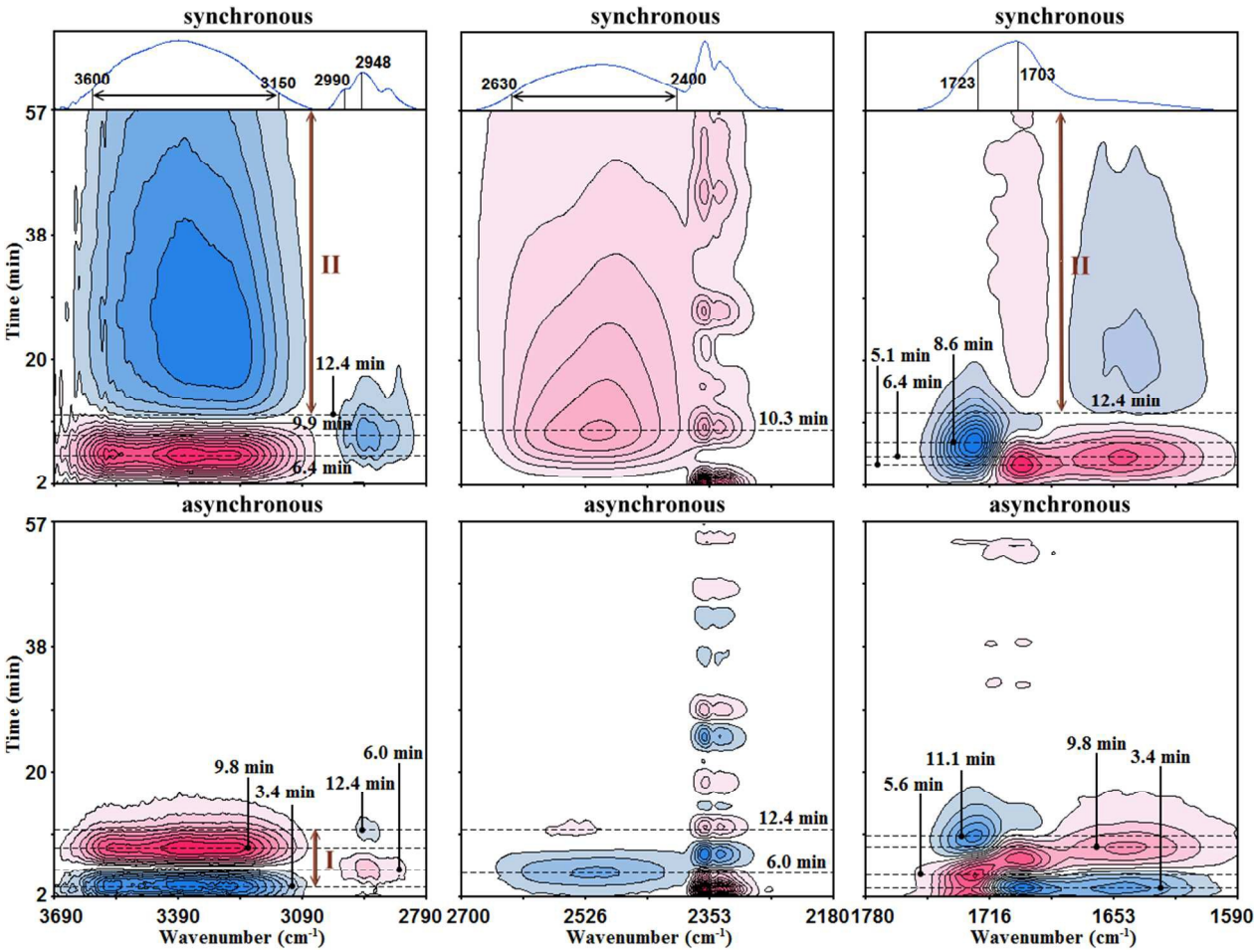

Figure 3. PCMW2D correlation ATR-FTIR spectra in the regions of 3690-2790 cm^{-1}, 2700-2180 cm^{-1}, and 1780-1590 cm^{-1} calculated from the time-dependent ATR-FTIR spectroscopy. The top is synchronous spectra, and the bottom is asynchronous spectra. In the synchronous spectra, the horizontal dashed lines represent the time points at 5.1 min, 6.4 min, 8.6 min, 9.9 min, and 12.4 min. In the asynchronous spectra, the horizontal dashed lines correspond to the time points 3.4 min, 5.6 min, 6.0 min, 9.8 min, 11.1 min, and 12.4 min, respectively. The pink areas represent positive correlation intensity, and the sky blue areas represent the negative.

3.2. Time regions determined from PCMW2D

PCMW2D correlation ATR-FTIR spectra of D_2O diffusion into the PHEMA-based contact lens in the regions of 3700-2800 cm^{-1}, 2700-2180 cm^{-1}, and 1780-1600 cm^{-1} are shown in **Figure 3**, which are calculated from the time-dependent ATR-FTIR spectroscopy from 0 to 60 min. PCMW2D contains synchronous and asynchronous correlation spectra. The pink areas represent positive correlation intensity, and the sky blue areas represent the negative correlation intensity. For synchronous FTIR spectra, the positive correlation intensity indicates the increasing of the spectral intensity at a given wavenumber in the time-dependent ATR-FTIR spectroscopy, and vice versa[54]. In **Figure 3**, for synchronous ATR-FTIR spectra, the bands of 2630-2400 cm^{-1} which is assigned to ν(O−D) of D_2O shows a broad positive correlation peak throughout the entire time range, indicating the continuous penetration of D_2O into the contact lens. Here, the time point of D_2O diffusing into is observed at 10.3 min, and this reveals that the penetration rate of D_2O is the maximum at 10.3 min after starting the ATR-FTIR experiment. The bands of 2990 cm^{-1} and 2948 cm^{-1} appear a negative correlation peak at 9.9 min, which indicates the hydration process of $-CH_3$ and $-CH_2-$ groups. A negative correlation peak of 1723 cm^{-1} (ν(C=O, free)) is also observed at 8.6 min, revealing the concentration reduction of "free" C=O in the contact lens. However, the bands of 3600-3150 cm^{-1}, 1703 cm^{-1}, and 1660-1610 cm^{-1} appear two correlation peaks throughout the entire time range. Specifically, both 3600-3150 cm^{-1} and 1660-1610 cm^{-1} show a positive correlation peak at 6.4 min and a broad negative correlation peak within 12.4-57 min. Similarly, 1703 cm^{-1} (ν(C=O, bonded)) shows a positive correlation peak at 5.1 min and a broad positive correlation peak within 12.4-57 min. 3600-3150 cm^{-1} and 1660-1610 cm^{-1} are assigned to ν(O−H) and δ(O−H) in the contact lens, respectively. As mentioned above, in synchronous ATR-FTIR spectra, the positive correlation intensity indicates the increasing of spectral intensity at a specific wavenumber in the time-dependent ATR-FTIR spectra, and vice versa. Thus, combining with the discussion in the above section, it clearly

reveals that O−H groups in the contact lens undergo two processes in the presence of D_2O. The first process is the hydrogen bonds formation of O−H groups, certainly between "free" O−H and infiltrated D_2O. The second process is the hydrogen bonds breaking of O−H groups, probably between two O−H groups or between O−H and C=O in the cross-linked PHEMA. Similarly, the hydrogen-bonded C=O in the contact lens also shows two processes of the concentration increasing at 5.1 min and within 12.4-57 min, respectively. In synchronous ATR-FTIR spectra, it can be determined that the PHEMA-based contact lens presents two processes during D_2O penetrating into. It is also noted that 12.4 min is the dividing line between these two processes.

The asynchronous spectra can be easily used to determine the time (or temperature) region of polymer transitions.[40-46] As shown in **Figure 3**, for the first process, the time regions of the bands of 3600-3150 cm^{-1} and 1660-1610 cm^{-1} are both accurately determined within 3.4-9.8 min. The time regions of the bands of 2990 cm^{-1}, 2948 cm^{-1} and 2630-2400 cm^{-1} are observed within 6.0-12.4 min. Similarly, the time region of 1723 cm^{-1} is determined within 5.6-11.1 min. For the first process, for convenience, the lowest point 3.4 min of these time regions is used as the onset point, and the highest point 12.4 min is used the ending point. So, the whole time region of the first process is easily defined as 3.4-12.4 min, as labelled in **Figure 3**. For the second process, because the time region cannot be determined from asynchronous ATR-FTIR spectra, we directly use the dividing line in synchronous ATR-FTIR spectra to define this region as 12.4-57.0 min, also labelled in **Figure 3**. Here, these two processes are named as process I and process II.

Figure 4 illustrates the spectral intensity change of the time-dependent ATR-FTIR at 3390 cm^{-1}, 2990 cm^{-1}, 2948 cm^{-1}, 2510 cm^{-1}, 1723 cm^{-1}, and 1703 cm^{-1} from 0 to 60 min. The vertical dashed lines represent the time points at 3.4 min, 12.4 min, and 57.0 min, which correspond to the onset point and the ending point of process I and process II determined from PCMW2D. It is noted that, as denoted by "cross" symbol, the time point at 3.4 min is just the initial point of the bands intensity increasing of D_2O (2510 cm^{-1}). Meanwhile, the bands intensities of 3390 cm^{-1}, 2990 cm^{-1}, 2948 cm^{-1}, 1723 cm^{-1}, and 1703 cm^{-1} also begin to change from 3.4 min. This shows that D_2O spends 3.4 min penetrating into the contact lens, and then the interactions between D_2O and the functional groups of the cross-linked PHEMA immediately take place. The time point at 12.4 min is the inflection point of the bands intensity curves of 3390 cm^{-1}, 2990 cm^{-1}, 2948 cm^{-1}, 1723 cm^{-1}, and 1703 cm^{-1}. Within 3.4-12.4 min, the spectral intensities of 3390 cm^{-1} and 1703 cm^{-1} increases with the time extending, and those of 2990 cm^{-1}, 2948 cm^{-1}, and 1723 cm^{-1} decrease at the same time. However, after 12.4 min (the inflection point), a sudden rapid decrease of the spectral intensity of 3390 cm^{-1} is observed, and the intensities of 2990 cm^{-1} and 2948 cm^{-1} gradually drop to the lowest value and remain constant. We also observe the slow increase of spectral intensity at 1703 cm^{-1} within 12.4-57.0 min. It is noted that no inflection point appears at 12.4 min for D_2O intensity curve (2510 cm^{-1}), and the intensity of 2510 cm^{-1} steadily increases from 3.4 to 57.0 min, revealing the continuous penetration of D_2O into the contact lens. **Figure 4** clearly shows that the PHEMA-based contact lens undergoes two interaction processes after D_2O penetrating into. The above discussion also approves the time regions determined from PCMW2D are correct and reasonable.

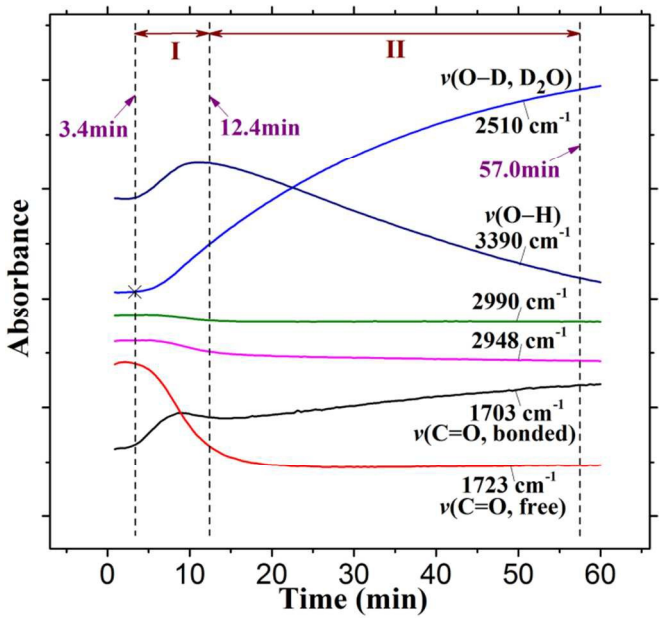

Figure 4. Spectral intensity change of the time-dependent ATR-FTIR at 3390 cm^{-1}, 2990 cm^{-1}, 2948 cm^{-1}, 2510 cm^{-1}, 1723 cm^{-1}, and 1703 cm^{-1} from 0 to 60 min.

From PCMW2D correlation ATR-FTIR spectra (**Figure 3**), combining with **Figure 4**, the following information can be preliminarily summarized. For process I (3.4-12.4 min), D_2O takes 3.4 min to penetrate into the contact lens after the ATR-FTIR experiment starting. The hydrogen bonds between D_2O and "free" O−H in the cross-linked PHEMA are immediately generated. Meanwhile, the hydrogen bonds between D_2O and "free" C=O in the cross-linked PHEMA are also immediately formed, resulting in the concentration increase of hydrogen-bonded C=O groups. The $-CH_3$ and $-CH_2-$ groups of the cross-linked PHEMA are gradually surrounded by a number of D_2O molecules, and a hydration process of $-CH_3$ and $-CH_2-$ occurs. Consequently, the dry contact lens is transformed into a typical PHEMA-based hydrogel. For process II (12.4-57.0 min), D_2O still continuously penetrates into the contact lens. A sudden hydrogen bonds breaking of bonded O−H groups is clearly observed, and the concentration of hydrogen-bonded C=O groups still slowly increases. Although two processes of the water absorption of the contact lens are determined, and some rough information of these two processes is obtained from the above discussion, the microdynamics mechanism is still unclear. Therefore, 2D correlation analysis for process I and process II is necessary.

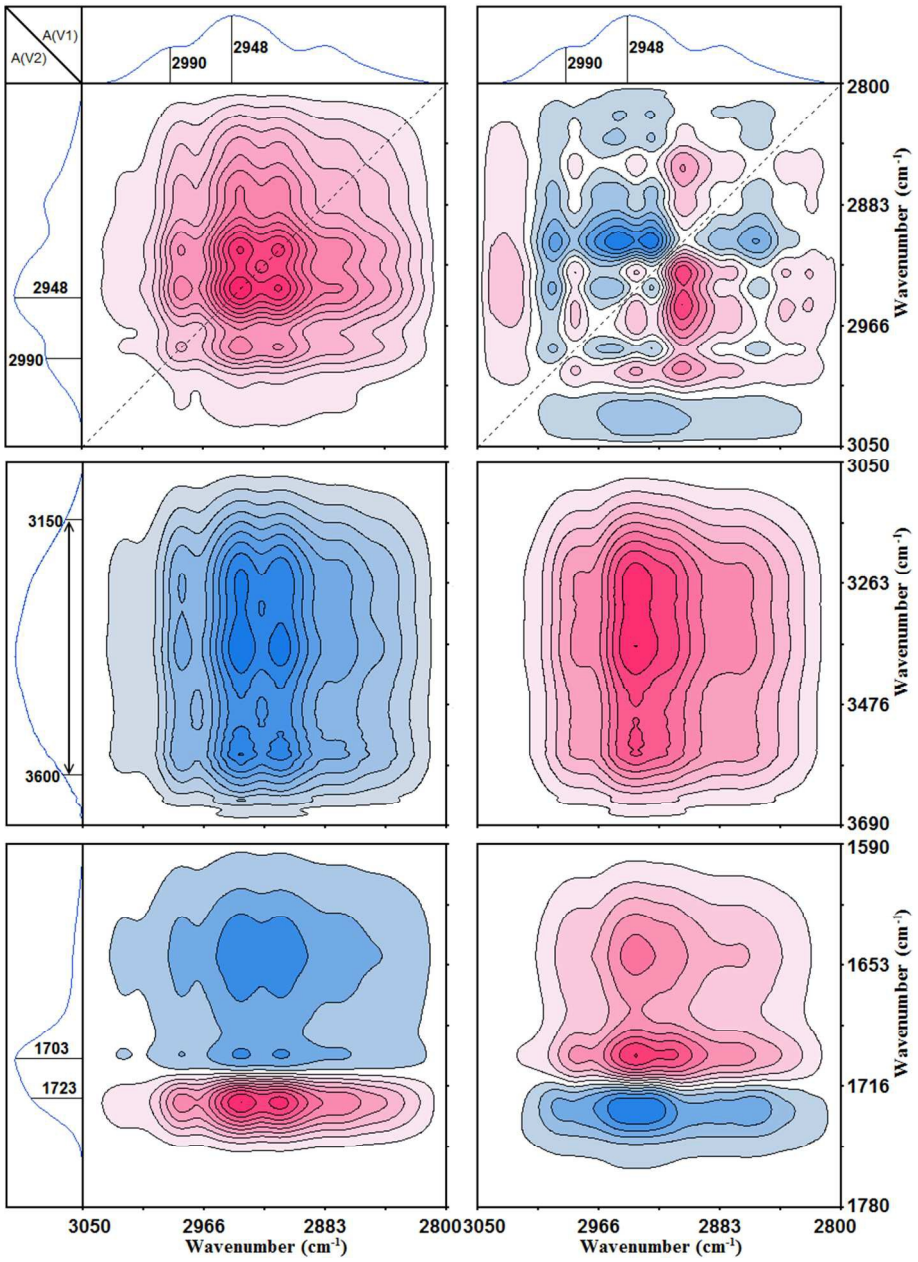

Figure 5. Synchronous (left) and asynchronous (right) ATR-FTIR spectra calculated from the time-dependent ATR-FTIR spectra of process I (3.4-12.4 min) in the regions of 3050-2800 cm^{-1}, 3050-2800 cm^{-1} *vs* 3690-3050 cm^{-1}, and 3050-2800 cm^{-1} *vs* 1780-1590 cm^{-1}. Pink and sky blue areas represent the positive and negative correlation intensity, respectively.

3.3. Generalized 2D correlation analysis

The time-dependent ATR-FTIR spectra of process I (3.4-12.4 min) and process II (12.4-57 min) were used to perform the generalized 2D correlation analysis. Generalized 2D FTIR spectra also contain synchronous and asynchronous spectra. The sequential order of the spectral intensity change at a given wavenumber can be conveniently judged by the sign of the correlation peaks using Noda's rules.[55]

3.3.1. Process I

The generalized 2D correlation ATR-FTIR spectra calculated from the time-dependent ATR-FTIR spectra of process I (3.4-12.4 min) in the regions of 3050-2800 cm^{-1}, 3050-2800 cm^{-1} *vs* 3690-3050 cm^{-1}, 3050-2800 cm^{-1} *vs* 1780-1590 cm^{-1}, 1780-1590 cm^{-1}, and 1780-1590 cm^{-1} *vs* 3690-3050 cm^{-1} are shown in **Figure 5** and **Figure 6**. The left is the synchronous spectra, and the right is the asynchronous spectra. In **Figure 5** and **Figure 6**, the pink areas represent positive correlation intensity, and the sky blue areas represent the negative.

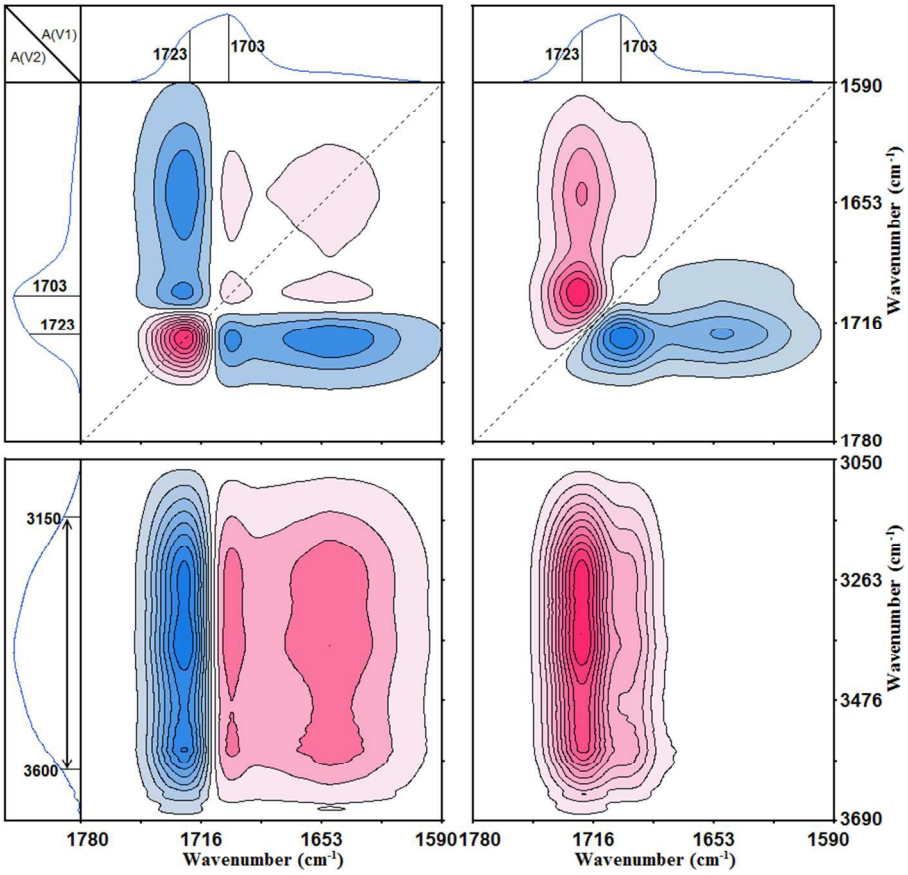

Figure 6. Synchronous (left) and asynchronous (right) ATR-FTIR spectra calculated from the time-dependent ATR-FTIR spectra of process I (3.4-12.4 min) in the regions of 1780-1590 cm^{-1}, and 1780-1590 cm^{-1} *vs* 3690-3050 cm^{-1}.

The sign of the cross peaks at (2990 cm^{-1}, 2948 cm^{-1}), (2948 cm^{-1}, 3600-3150 cm^{-1}), (2990 cm^{-1}, 3600-3150 cm^{-1}), (2990 cm^{-1}, 1703 cm^{-1}), (2948 cm^{-1}, 1703 cm^{-1}), (2990 cm^{-1}, 1723 cm^{-1}), (2948 cm^{-1}, 1723 cm^{-1}), (1723 cm^{-1}, 1703 cm^{-1}), (1703 cm^{-1}, 3600-3150 cm^{-1}), and (1723 cm^{-1}, 3600-3150 cm^{-1}) are summarized in **Table 2**. According to Noda's rules, the sequential order is 1703 cm^{-1}→3600-3150 cm^{-1}→1723 cm^{-1}→2990 cm^{-1}→2948 cm^{-1}. Here, the symbol "→" represents "before", and "←" represents "after". The corresponding sequential order of the functional groups in the contact lens is ν(C=O, bonded)→ν(O−H)→ν(C=O, free)→ν_{as}(−CH_3, hydrated)→ν_{as}(−CH_2−, hydrated).

This clearly shows that the first step of process I is the generation of O−D···O=C hydrogen bonds between D_2O and a part of "free" carbonyl groups in the contact lens, and then the second step is the hydrogen bonding of D_2O with "free" hydroxyl groups to form O−D···O−H structure. The third step is also the hydrogen bonds generation between D_2O and some of "free" carbonyl groups. However, the type of these "free" carbonyl groups is different from those in the first step. As shown in **Scheme 1**, there exist two types of "free" carbonyl groups in the dry contact lens. The first type is the "free" carbonyl groups in PHEMA side chains, and the second type is "free" carbonyl groups of the crosslinking agent which is close to the crosslinking points. The "free" carbonyl groups in the third step are the second type. Obviously, the "free" carbonyl groups of the first type have a more capacity of movement, and therefore, D_2O is preferentially to form the hydrogen bonds with "free" carbonyl groups of the first type. However, the movement of the "free" carbonyl groups of the second type is difficult, and it also exists a large steric hindrance of the surrounding environment. So, after D_2O forming hydrogen bonds with "free" hydroxyl groups in the side chains in the contact lens, D_2O subsequently penetrates and moves to the areas of the "free" C=O of the second type, and then the hydrogen bonds of D_2O and these "free" C=O are generated. After that, the fourth step is the hydration process of −CH_3 groups by D_2O, and the last step is the hydration process of −CH_2− groups in the cross-linked PHEMA.

According to the research of Morita,[56] about 47.3% of O−H groups in PHEMA side chain ends are hydrogen-bonded with C=O groups, while the rest of O−H groups are generated the hydrogen bonds of O−H···O−H type. That means, about 52.7% C=O groups in PHEMA side chains exists as the "free" state, and O−H groups are almost all hydrogen-bonded. However, in the present study, the used PHEMA-based contact lens are partly cross-linked, and therefore the movement ability of the molecular chains are restricted due to the existence of the cross-linking points, resulting in part of the "free" C=O groups being unable to form hydrogen bonds with O−H groups. Here,

it can be naturally inferred that the amount of the "free" C=O groups in PHEMA side chains is bigger than 52.7%, and some of the O−H groups certainly exist as the "free" state. The number of "free" C=O groups in the contact lens are much larger than that of "free" O−H groups. So, in process I, D_2O is firstly hydrogen-bonded with "free" C=O groups in PHEMA side chains, and then bonded with "free" O–H groups.

Table 2. Sequential orders of the bands of the hydrated $-CH_3$, the hydrated $-CH_2-$, O−H, "free" C=O, hydrogen-bonded C=O groups in the PHEMA-based contact lens, and their cross regions gained from **Figure 5** and **Figure 6**.

Cross correlation peak (cm^{-1}, cm^{-1})	Sign in synchronous spectra	Sign in asynchronous spectra	Sequential order
(2990, 2948)	+	+	2990→2948
(2948, 3600-3150)	-	+	2948←(3600-3150)
(2990, 3600-3150)	-	+	2990←(3600-3150)
(2990, 1703)	-	+	2990←1703
(2948, 1703)	-	+	2948←1703
(2990, 1723)	+	-	2990←1723
(2948, 1723)	+	-	2948←1723
(1723, 1703)	-	+	1723←1703
(1703, 3600-3150)	+	+	1703→(3600-3150)
(1723, 3600-3150)	-	+	1723←(3600-3150)
1703 cm^{-1}→(3600-3150) cm^{-1}→1723 cm^{-1}→2990 cm^{-1}→2948 cm^{-1}			
ν(C=O, bonded)→ν(O−H)→ν(C=O, free)→ν_{as}($-CH_3$, hydrated)→ν_{as}($-CH_2-$, hydrated)			

According to 2D correlation analysis, the fourth step is determined as the hydration process of $-CH_3$ groups, and the last step is the hydration process of $-CH_2$ groups. It can be also observed in **Figure 4** that the bands intensities of $-CH_3$ (2990 cm^{-1}) and $-CH_2-$ groups (2948 cm^{-1}) gradually decrease in process I. However, theoretically, the intensity of these two bands should be increased due to the concentration enrichment of hydrated $-CH_3$ and $-CH_2-$ groups. This arouses our interest. A similar phenomenon was observed by other scientists when applied ATR-FTIR technique to study the polymer/water systems. For examples, Tang et al. studied the water diffusion in a positively charged membrane. She found the characteristic bands intensity of the aromatic stretching vibration decreased, and attributed this phenomenon to the swelling of the film.[38] Kitano and his coworkers investigated the water structure in polymethoxyethylacrylate (PMEA) film by using ATR-FTIR spectroscopy, and a similar result was obtained. They attributed this phenomenon to the presence of water molecules in the vicinity of hydrocarbon moieties in the polymer films.[57]

However, in our opinion, there are two possible reasons leading this phenomenon to occur. The first reason is the swelling of the polymer film by water sorption, just like what Tang et al. considered.[36] This is because the technique of ATR-FTIR probes the interface of the polymer membrane tightly attached to the optical crystal. As the water diffusing in, the polymer membrane is gradually swelled, and the average number of the functional groups in polymers in a unit volume at the interface is decreased with the swelling of the membrane, causing the reduction of the ATR-FTIR absorption intensity. The second reason is the change of the refractive index during the water sorption process.[58] According to the literature, the refractive index of water in the mid-infrared region is below to 1.33,[59] which is usually smaller than that of polymers. Thus, the refractive index of the polymer absorbed water is smaller than that of the dried polymer. In general, the refractive index of the sample has a great influence on the penetration depth (d_p) of the infrared light, as shown in equation (1).

$$d_p = \frac{\lambda}{2\pi n_p \sqrt{sin^2\theta - (n_s/n_p)^2}} \quad (1)$$

where λ is the wavelength of the infrared light in the optical crystal, and n_s and n_p are the refractive indices of the sample and the optical crystal, respectively. The parameter θ is the incidence angle of the infrared light. From equation (1), it can be inferred that a smaller refractive index of the sample gives a smaller penetration depth of the infrared light, and a smaller penetration depth means fewer functional groups of the membrane are detected. Therefore, the bands intensities of $-CH_3$ (2990 cm^{-1}) and $-CH_2-$ groups (2948 cm^{-1}) gradually decrease with the time extending in the present study.

3.3.2. Process II

The generalized 2D correlation ATR-FTIR spectra calculated from the time-dependent ATR-FTIR spectra of process II (12.4-57.0 min) in the regions of 1780-1580 cm^{-1} and 1780-1580 cm^{-1} *vs* 3690-3050 cm^{-1} are shown in **Figure 7**. In **Figure 4**, it can be observed that the intensities of $-CH_3$ (2990 cm^{-1}) and $-CH_2-$ groups (2948 cm^{-1}) gradually drop to the lowest value in process I and remain constant in process II. That is to say, the bands intensities of $-CH_3$ and $-CH_2-$ groups have no change at all. So, the generalized 2D correlation ATR-FTIR analysis for $-CH_3$ and $-CH_2-$ groups was not performed in process II. The sign of the cross peaks at (1723 cm^{-1}, 1703 cm^{-1}), (1703 cm^{-1}, 3600-3150 cm^{-1}) and (1723 cm^{-1}, 3600-3150 cm^{-1}) are summarized in **Table 3**. According to Noda's rules, the sequential order is 1723 cm^{-1}→(3600-3150) cm^{-1}→1703 cm^{-1}. The corresponding sequential order of functional groups is ν(C=O, free)→ν(O−H)→ν(C=O, bonded). This shows that the first step of process II is also the hydrogen bonds generation between D_2O and "free" C=O groups just like the first step of process I, and the second step is related to O−H groups, probably the hydrogen bonds breaking of bonded O−H groups. The last step is associated with the bonded C=O groups.

The O−H groups are involved in the second step of both process I and process II. The bands intensity of O−H groups increases in process I, revealing the hydrogen bonds generation between D_2O and "free" O−H groups in the side chains in the contact lens. However, in process II, a sharp decrease of the bands intensity of O−H groups is observed. What causes this phenomenon? Whether it is caused by the swelling of the contact lens or the refractive index change as

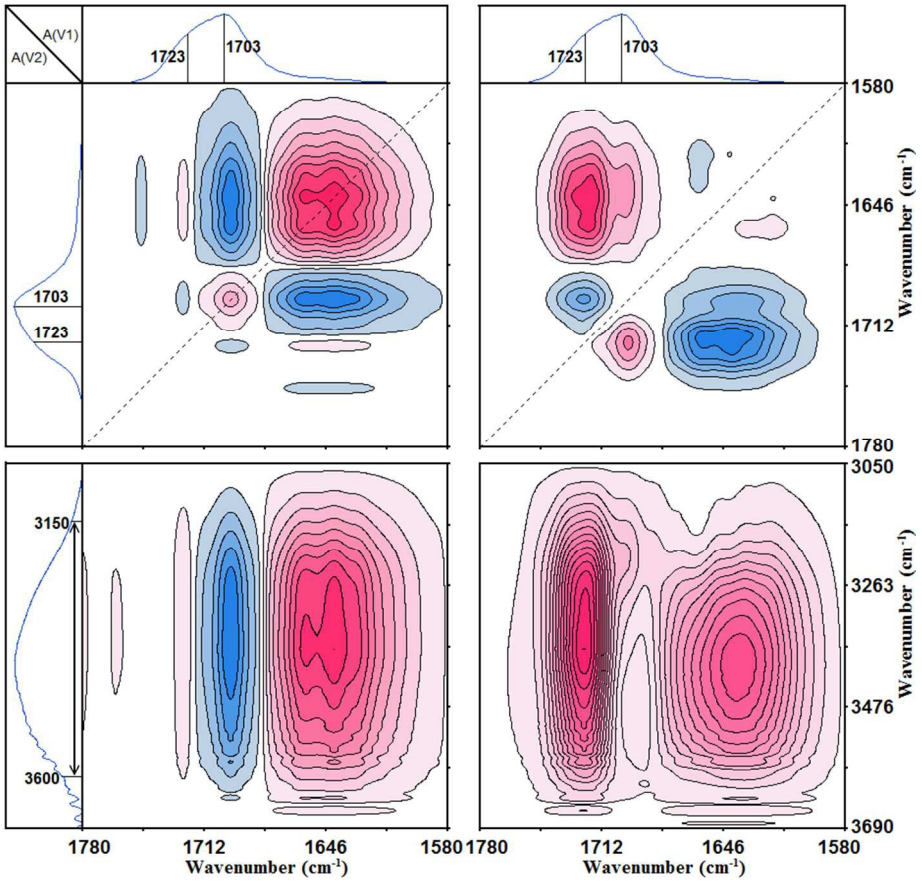

Figure 7. Synchronous (left) and asynchronous (right) ATR-FTIR spectra calculated from the time-dependent ATR-FTIR spectra of process II (12.4-57.0 min) in the regions of 1780-1580 cm^{-1} and 1780-1580 cm^{-1} *vs* 3690-3050 cm^{-1}.

mentioned above, just like $-CH_3$ and $-CH_2-$ groups in the fourth and fifth steps of process I. In process II, the bands intensities of $-CH_3$ (2990 cm^{-1}) and $-CH_2-$ groups (2948 cm^{-1}) remain unchanged. If the bands intensity decrease of O−H groups is caused by the lens swelling or the reduction of the refractive index, the bands intensity of $-CH_3$ and $-CH_2-$ groups should also be reduced. That is to say, the bands intensity decrease of O−H groups is caused by other reasons. Because of O−H groups containing the active hydrogen, we think it is probably attributed to a deuterium exchange between D_2O and O−H groups in the contact lens. Specifically, the intra-molecular hydrogen bonds O−H···O=C or O−H···O−H in the cross-linked PHEMA are broken due to the induction of the surrounding D_2O molecules, and then the D atom replace the H atom in O−H groups to form a new O−D. Both the hydrogen bonds breaking of O−H···O=C or O−H···O−H and the deuterium exchange will lead to the bands intensity decrease of O−H groups. Therefore, the second step of process II is the hydrogen bonds breaking of bonded O−H groups and the deuterium exchange between D_2O and O−H.

Table 3. Sequential orders of the bands of O−H, "free" C=O, hydrogen-bonded C=O groups in the PHEMA-based contact lens, and their cross regions gained from **Figure 7**.

Cross correlation peak (cm^{-1}, cm^{-1})	Sign in synchronous spectra	Sign in asynchronous spectra	Sequential order
(1723, 1703)	-	-	1723→1703
(1703, 3600-3150)	-	+	1703←(3600-3150)
(1723, 3600-3150)	+	+	1723→(3600-3150)
1723 cm^{-1}→ (3600-3150) cm^{-1}→1703 cm^{-1}			
v(C=O, free)→*v*(O−H)→*v*(C=O, bonded)			

According to 2D correlation analysis, the third step of process II is related to the bonded C=O groups, and the bands intensity of bonded C=O groups (1703 cm^{-1}) slowly increases in process II, as shown in **Figure 4**. It is noted that the bands intensity of "free" C=O groups (1703 cm^{-1}) has no apparent change in process II, which indicates the concentration increase of the bonded C=O groups is not contributed from the transformation of the "free" C=O groups. Similarly, such as the second step, we think this step still has a relationship with the deuterium exchange. After the breaking of the O−H···O=C structure and the deuterium exchange between D_2O and O−H, the dissociated C=O groups reforms hydrogen bonds with the new generated O−D. Therefore, the third step of process II is

the hydrogen bonds generation between the dissociated C=O groups (in the second step) and the new generated O−D.

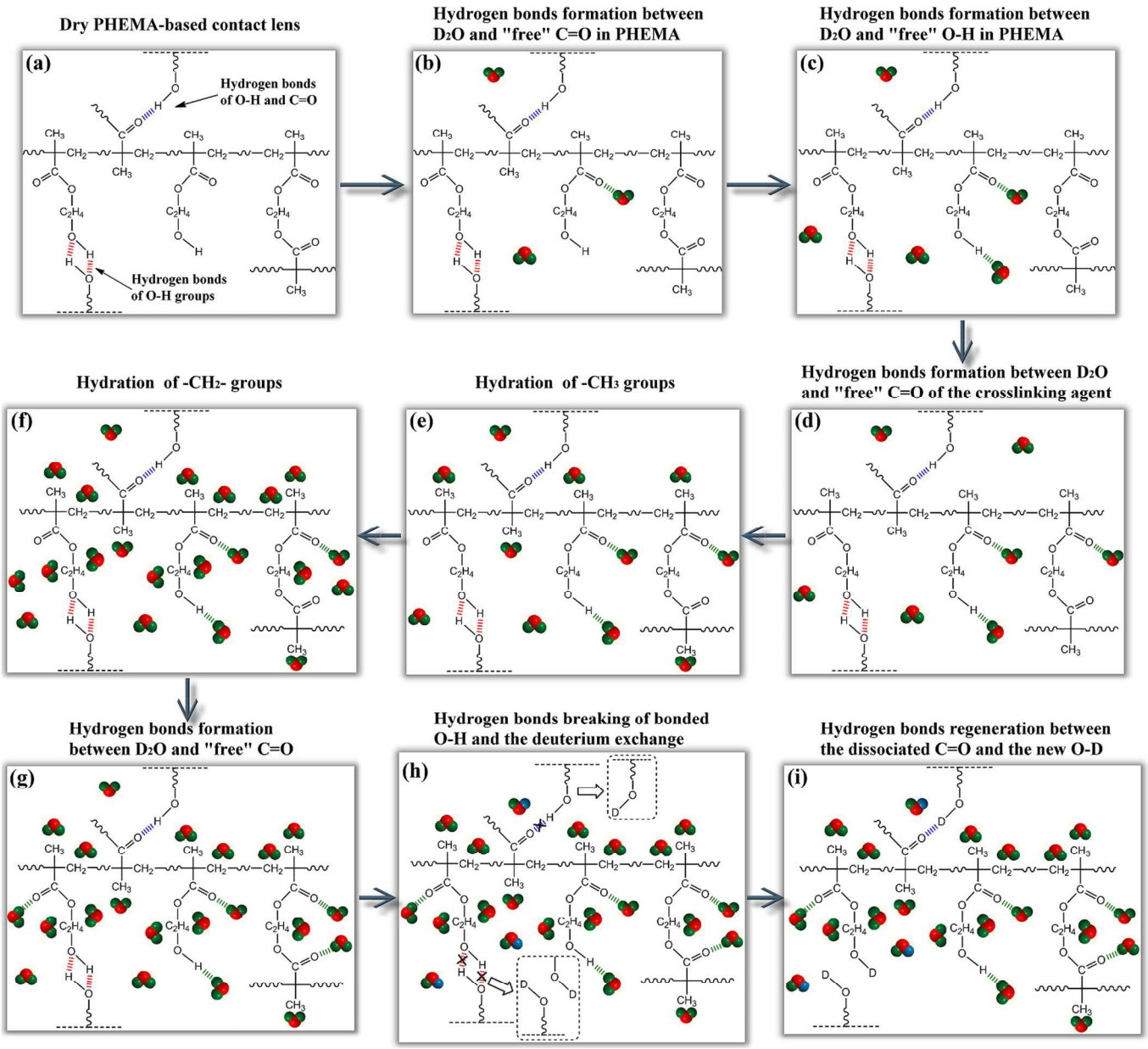

Scheme 2. Detailed steps of process I and process II inferred from the 2D correlation analysis. **(a)** PHEMA-based contact lens of the dry state; **(b)-(f)** belong to process I (3.4-12.4 min) which undergoes 5 steps; **(g)-(i)** belong to process I (12.4-57.0 min) which has 3 steps. D_2O molecules are represented by the 3D spherical model. The red balls are oxygen (O) atoms, and the green balls are deuterium (D) atoms. The hydrogen bonds of O−H···O−H and O−H···O=C in the contact lens are marked as red and blue, respectively. The hydrogen bonds between the contact lens (O=C or O−H) and D_2O are marked as green.

The detailed steps of process I and process II inferred from the 2D correlation analysis are illustrated in **Scheme 2**. Process I (3.4-12.4 min) has 5 steps, and process II (12.4-57 min) has 3 steps. In **Scheme 2**, D_2O molecules are represented by the 3D spherical model. The red balls are oxygen (O) atoms, and the green balls are deuterium (D) atoms. The hydrogen bonds of O−H···O−H and O−H···O=C in the contact lens are marked as red and blue, respectively. The hydrogen bonds between the contact lens (O=C or O−H) and D_2O are marked as green. **Scheme 2(a)** is the PHEMA-based contact lens of the dry state. **Scheme 2(b)-2(f)** belongs to process I, and **Scheme 2(g)-2(i)** belong to process II. For the dry contact lens, there exists two types of hydrogen bonds structure (O−H···O−H and O−H···O=C), and $-CH_2-$, $-CH_3$ groups are fully dehydrated. After D_2O diffusing into the contact lens, for process I, the first step is the D_2O molecules hydrogen-bonding with "free" −C=O groups in the side chains of PHEMA segments. The second step is the hydrogen bonds formation of O−H···O−D structure between D_2O and "free" O−H groups in the side chain ends. The "free" O−H groups in the cross-linked PHEMA are almost exhausted in this step due to the small amount. The third step is the hydrogen bonds

generation of D_2O and the "free" C=O groups of the crosslinking agent which is close to the crosslinking points in the contact lens. Because of a poor movement capacity of chain segments and a large steric hindrance, D_2O penetrates and moves close to theses "free" C=O groups later. After that, with the time extending, more and more D_2O molecules gathered around the alkyl groups of the cross-linked PHEMA. Consequently, the fourth step is the hydration process of $-CH_3$ groups by D_2O, and the fifth step is the hydration process of $-CH_2-$ groups. For process II, the first step is the same as that of process I, resulting in the "free" C=O groups in the contact lens are almost all hydrogen-bonded with D_2O molecules. The second step is the hydrogen bonds breaking of bonded O−H groups (O−H···O=C or O−H···O−H) in the PHEMA-based contact lens and the deuterium exchange between D_2O and O−H groups in the side chain ends, resulting in the formation of the new O–D groups in the contact lens. The third step is also the result of the deuterium exchange, which is the hydrogen bonds regeneration between the dissociated C=O groups (in the second step) and the new generated O−D.

4. Conclusions

In this study, the time-dependent ATR-FTIR spectroscopy combining with PCMW2D and 2D correlation analysis was used to study the microdynamics mechanism of D_2O absorption of the PHEMA-based contact lens.

PCMW2D correlation ATR-FTIR spectra revealed that D_2O spent 3.4 min to penetrate into the contact lens after the ATR-FTIR experiment starting. After that, D_2O continuously penetrated into the contact lens throughout the entire time range of the ATR-FTIR experiment. PCMW2D also revealed that the PHEMA-based contact lens underwent two processes (named as I and II) during D_2O absorption, and time regions of process I and process II are 3.4-12.4 min and 12.4-57.0 min, respectively.

The 2D correlation analysis was performed for process I and process II. According to the sequential order of the functional groups, it was approved that process I (3.4-12.4 min) has 5 steps, and process II (12.4-57 min) has 3 steps. For process I, the first step is the D_2O molecules hydrogen-bonding with "free" −C=O groups in the side chains. The second step is the hydrogen bonds generation of O−H···O−D structure between D_2O and "free" O−H groups in the side chain ends. The third step is the hydrogen bonds generation of D_2O and the "free" C=O groups of the crosslinking agent which is close to the crosslinking points in the contact lens. The fourth and the fifth steps are the hydration of $-CH_3$ and $-CH_2-$ groups by D_2O, respectively. After above 5 steps, the dry contact lens was transformed into a typical cross-linked PHEMA hydrogel. For process II, the first step is the same as that of process I. The second step is the hydrogen bonds breaking of bonded O−H groups in the contact lens and the deuterium exchange between D_2O and O−H groups in the side chain ends. The third step is also the result of the deuterium exchange, which is the hydrogen bonds reformation between the dissociated C=O groups and the new O−D.

Acknowledgements

This work was supported by the National Natural Science Foundation of China (Grant Nos. 51473104, 51003066) and State Key Laboratory of Polymer Materials Engineering (Grant No. sklpme2014-3-06, sklpme2014-2-10).

Notes and references

[a] State Key Laboratory of Polymer Materials Engineering of China, Polymer Research Institute, Sichuan University, Chengdu 610065, China

*Corresponding author. Tel.: +86-28-85402601; Fax: +86-28-85402465; E-mail address: zhoutaopoly@scu.edu.cn (T. Zhou)

1. O. Wichterle and D. Lim, *Nature*, 1960, 185, 117-118.
2. P. C. Nicolson and J. Vogt, *Biomaterials*, 2001, 22, 3273-3283.
3. S.-D. Lee, G.-H. Hsiue, C.-Y. Kao and P. C.-T. Chang, *Biomaterials*, 1996, 17, 587-595.
4. C.-D. Young, J.-R. Wu and T.-L. Tsou, *Biomaterials*, 1998, 19, 1745-1752.
5. C. J. White, A. Tieppo and M. E. Byrne, *J. Drug Deliv. Sci. Tec.*, 2011, 21, 369-384.
6. S. Atzet, S. Curtin, P. Trinh, S. Bryant and B. Ratner, *Biomacromolecules*, 2008, 9, 3370-3377.
7. T. V. Chirila, Y.-C. Chen, B. J. Griffin and I. J. Constable, *Polym. Int.*, 1993, 32, 221-232.
8. P. M. Ladage, J. V. Jester, W. M. Petroll, J. P. G. Bergmanson and H. D. Cavanagh, *Eye Contact Lens*, 2003, 29, S2-S6.
9. N. A. Brennan, N. Efron, A. S. Bruce, D. I. Duldig and N. J. Russo, *Am. J. Optom. Physiol. Opt.*, 1988, 65, 277-281.
10. N. Efron, N. A. Brennan, A. S. Bruce, D. I. Duldig and N. J. Russo, *Eye Contact Lens*, 1987, 13, 152-156.
11. M. F. Refojo and F.-L. Leong, *Eye Contact Lens*, 1981, 7, 226-233.
12. Y.-M. Sun and H.-L. Lee, *Polymer*, 1996, 37, 3915-3919.
13. F. Fornasiero, M. Ung, C. J. Radke and J. M. Prausnitz, *Polymer*, 2005, 46, 4845-4852.
14. N. Efron and P. B. Morgan, *Eye Contact Lens*, 1999, 25, 148-151.
15. D. K. Martin, *J. Biomed. Mater. Res.*, 1995, 29, 857-865.
16. S. A. Little and A. S. Bruce, *Ophthalmic Physiol. Opt.*, 1994, 14, 65-69.
17. T. R. Golding, M. G. Harris, R. C. Smith and N. A. Brennan, *Acta Ophthalmologica Scandinavica*, 1995, 73, 139-144.
18. J. G. Wijmans and R. W. Baker, *J. Membr. Sci.*, 1995, 107, 1-21.
19. I. Fatt and T. K. Goldstick, *J. Colloid Sci.,* 1965, 20, 962-989.
20. F. Fornasiero, F. Krull, J. M. Prausnitz and C. J. Radke, *Biomaterials*, 2005, 26, 5704-5716.
21. M. V. Monticelli, A. Chauhan and C. J. Radke, *Curr. Eye Res.*, 2005, 30, 329-336.
22. M. F. Refojo, *J. Appl. Polym. Sci.*, 1965, 9, 3417-3426.
23. L. Ferreira, M. M. Vidal and M. H. Gil, *Int. J. Pharmaceut.*, 2000, 194, 169-180.
24. L. E. Nita, M. T. Nistor, A. P. Chiriac and I. Neamtu, *Ind. Eng. Chem. Res.*, 2012, 51, 7769-7776.

25. P. McConville and J. M. Pope, *Polymer*, 2000, 41, 9081-9088.
26. M. C. Thimmegowda, P. M. Sathyanarayana, G. Shariff, M. B. Ashalatha, R. Ramani and C. Ranganathaiah, *Phys. Status Solidi A*, 2002, 193, 257-270.
27. G. Gates, J. P. Harmon, J. Ors and P. Benz, *Polymer*, 2003, 44, 215-222.
28. L. Guan, M. E. G. Jiménez, C. Walowski, A. Boushehri, and J. M. Prausnitz, *J. Appl. Polym. Sci.*, 2011, 122, 1457-1471.
29. A. Arce, F. Fornasiero, O. Rodriguez, C. J. Radke and J. M. Prausnitz, *Phys. Chem. Chem. Phys.*, 2004, 6, 103-108.
30. H. Yoo, R. Paranji and G. H. Pollack, *J. Phys. Chem. Lett.*, 2011, 2, 532-536.
31. P. McConville, M. K. Whittaker and J. M. Pope, *Macromolecules*, 2002, 35, 6961-6969.
32. W. E. Roorda, J. A. Bouwstra, M. A. de Vries and H. E. Junginger, *Biomaterials*, 1988, 9, 494-499.
33. M. C. Thimmegowda, H. B. R. Kumar and C. Ranganathaiah, *J. Appl. Polym. Sci.*, 2004, 92, 1355-1366.
34. Y. Maréchal and A. Chamel, *J. Phys. Chem. B*, 1996, 100, 8551-8555.
35. M. Wang, P. Wu, S. S. Sengupta, B. I. Chadhary, J. M. Cogen and B. Li, *Ind. Eng. Chem. Res.*, 2011, 50, 6447-6454.
36. Y. Shen and P. Wu, *J. Phys. Chem. B*, 2003, 107, 4224-4226.
37. K. Ichikawa, T. Mori, H. Kitano, M. Fukuda, A. Mochizuki and M. Tanaka, *J. Polym. Sci. Pol. Phys.*, 2001, 39, 2175-2182.
38. B. Tang, P. Wu and H. W. Siesler, *J. Phys. Chem. B*, 2008, 112, 2880-2887.
39. K. Kunimatsu, B. Bae, K. Miyatake, H. Uchida and M. Watanabe, *J. Phys. Chem. B*, 2011, 115, 4315-4321.
40. I. Noda, *Appl. Spectrosc.*, 1993, 47, 1329-1336.
41. I. Noda and Y. Ozaki, *Two-dimensional correlation spectroscopy: applications in vibrational and optical spectroscopy*, John Wiley & Sons, 2005.
42. X. Liu, T. Zhou, Y. Liu, A. Zhang, C. Yuan and W. Zhang, *RSC Adv.*, 2015, 5, 10231-10242.
43. Z. Wang and P. Wu, *RSC Adv.*, 2012, 2, 7099-7108.
44. Q. Yuan, T. Zhou, L. Li, J. Zhang, X. Liu, X. Ke and A. Zhang, *RSC Adv.*, 2015, 5, 31153-31165.
45. H. Lai, Z. Wang and P. Wu, *RSC Adv.*, 2012, 2, 11850-11857.
46. S. Morita, H. Shinzawa, I. Noda and Y. Ozaki, *Appl. Spectrosc.*, 2006, 60, 398-406.
47. M. Thomas and H. H. Richardson, *Vib. Spectrosc.*, 2000, 24, 137-146.
48. F. Fornasiero, J. M. Prausnitz and C. J. Radke, *J. Membr. Sci.*, 2006, 275, 229-243.
49. S. H. Kim, A. Opdahl, C. Marmo and G. A. Somorjai, *Biomaterials*, 2002, 23, 1657-1666.
50. H. Wang, S. Sun and P. Wu, *J. Phys. Chem. B*, 2011, 115, 8832-8844.
51. P. Schmidt, J. Dybal and M. Trchová, *Vib. Spectrosc.*, 2006, 42, 278-283.
52. B. J. Sun, Y. N. Lin, P. Y. Wu and H. W. Siesler, *Macromolecules*, 2008, 41, 1512-1520.
53. S. Morita, S. Ye, G. Li and M. Osawa, *Vib. Spectrosc.*, 2004, 35, 15-19.
54. S. Sun and P. Wu, *Soft Matter*, 2011, 7, 6451-6456.
55. I. Noda, A. E. Dowrey, C. Marcott, G. M. Story and Y. Ozaki, *Appl. Spectrosc.*, 2000, 54, 236A-248A.
56. S. Morita, K. Kitagawa and Y. Ozaki, *Vib. Spectrosc.*, 2009, 51, 28-33.
57. H. Kitano, K. Ichikawa, M. Fukuda, A. Mochizuki and M. Tanaka, *J. Colloid Interface Sci.,*, 2001, 242, 133-140.
58. S. Morita, M. Tanaka and Y. Ozaki, *Langmuir*, 2007, 23, 3750-3761.
59. J. E. Bertie and Z. Lan, *Appl. Spectrosc.*, 1996, 50, 1047-1057.

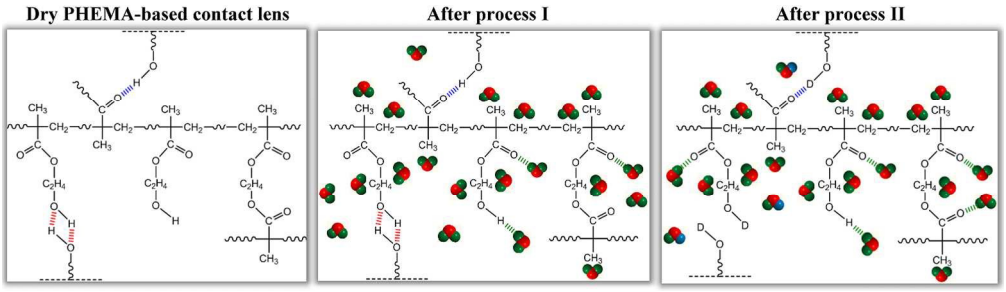

551x156mm (72 x 72 DPI)